A toy model for the effective density of acoustic metamaterials

Juliette Pierre, Valentin Leroy, Benjamin Dollet

PROCEEDINGS A

rspa.royalsocietypublishing.org

Research

Article submitted to journal

Subject Areas:
xxxxx, xxxxx, xxxx

Keywords:
xxxx, xxxx, xxxx

Author for correspondence:
Valentin Leroy
e-mail: valentin.leroy@u-paris.fr

A toy model for the effective density of acoustic metamaterials

Juliette Pierre[1], Valentin Leroy[2] and Benjamin Dollet[3]

[1]Sorbonne Univ., CNRS, 75005 Paris, France
[2]Univ. Paris Cité, CNRS, MSC, 75013 Paris, France
[3]Univ. Grenoble Alpes, CNRS, LIPhy, 38000 Grenoble, France

We propose a simple mechanical system that can be used as a toy model for calculating the effective density of acoustic metamaterials. Through analytical calculations, it gives a better understanding of how the effective density can become negative, when the system responds elastically instead of inertially. We show that this toy model can reproduce, qualitatively, the acoustical behaviour of some real acoustic metamaterials.

THE ROYAL SOCIETY PUBLISHING

1. Introduction

Metamaterials are structured materials for which exotic behaviours in terms of wave propagation emerge from the microstructure. The most striking example is probably that of metamaterials for electromagnetic waves having a negative refractive index [1], which is obtained when both the permittivity and permeability of the medium are negative. In acoustics, finding structures that lead to negative parameters has also been a fruitful field of research. The literature contains many examples of acoustic metamaterials with negative bulk modulus and/or negative density [2]. Among the countless resonant systems exhibiting such properties, one finds several studies on membrane or thin plate structures: simple membranes arranged in parallel or series [3–11], decorated membranes [12–15], thin plates loaded with small pillars [16], and also natural systems composed with liquid membranes [17].

However, the concept of negative density is still often unsettling when first encountered, much more than the idea of a negative compressibility or a negative permittivity. This is of course because the term of density can refer to the gravitational density, which cannot be negative, or to the inertial density, which can. The main motivation of the present article is to highlight the physical mechanisms underlying the negative effective density, in order to demythify this notion.

We propose a simple system that can be used as a toy model to understand the concept of effective density in acoustics. All the calculations are straightforward, based on Newton's second law, and we give some details about their derivations (sections 2 to 4), hopefully allowing scientists that are not familiar with metamaterials to gain a physical understanding of the mechanisms leading to negative density. With this toy model one can determine under which conditions a unit cell will give rise, or not, to a negative density (section 5), including in the case of dissipation (section 6). We also show that despite its crudeness, our toy model can reproduce, at least qualitatively, the acoustic behaviour of several existing metamaterials (section 7).

2. Effective mass

The system that we consider is sketched in Fig. 1. In an infinite tube of section $S=\pi R^2$, we consider an object made of an annulus (part 1) of mass M_1 and section S_1 around a disk (part 2) of mass M_2 and section S_2, both of thickness e. Parts 1 and 2 of this object are linked by a spring of stiffness K, and the ring is connected to the tube by a spring of stiffness K'. We note $z=0$ the position of the left face of the object, and $z=e$ that of its right face. The pressure difference between the left and right faces is noted ΔP and we are interested in the situation in which the system is harmonically excited: $\Delta P \exp(-\mathrm{i}\omega t)$.

For the simple case of a uniform mass M that slides without friction on the tube ($M_1=0$, $M_2=M$, $K=K'=0$) the displacement U is given by:

$$-M\omega^2 U = \Delta P S. \tag{2.1}$$

Note that the sign of U might seem counter-intuitive here: for $\Delta P>0$, one finds that $U<0$, which means that a pressure force that pushes to the right results in a displacement to the left. This is what is expected for a purely inertial response of the system: the system displacement is in antiphase with the excitation force.

In the general case with two masses, we define the effective mass, M_{eff}, as the ratio between the force $\Delta P S$ and the acceleration $-\omega^2\langle U\rangle$. The average displacement is defined as $\langle U\rangle=(1-x)U_1+xU_2$, where U_1 and U_2 are the displacements of masses 1 and 2, and $x=S_2/(S_1+S_2)$ is the surface fraction occupied by the central mass (mass 2). U_1 and U_2 are determined by solving the coupled equations

$$-M_1\omega^2 U_1 = \Delta P S_1 - K(U_1-U_2) - K'U_1 \tag{2.2}$$

$$-M_2\omega^2 U_2 = \Delta P S_2 - K(U_2-U_1). \tag{2.3}$$

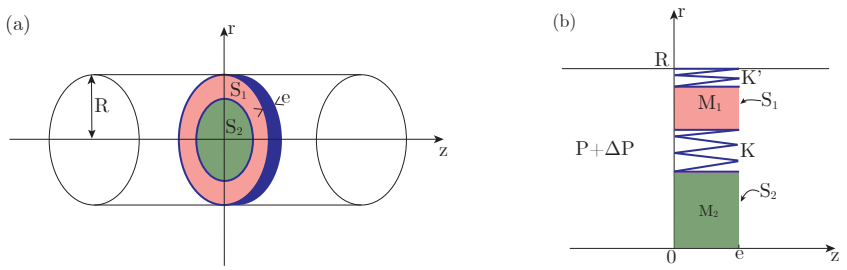

Figure 1. Schematic views of the system which we propose as a toy model. (a) An annulus of mass M_1 and surface S_1 is around a disk of mass M_2 and surface S_2, in an infinite tube of surface $S = S_1 + S_2 = \pi R^2$. (b) The two masses are connected via a spring K, and the annulus is linked to the tube with a spring K'. The effective mass of this system can be established by calculating how it moves when excited by an overpressure $\Delta P \exp(-\mathrm{i}\omega t)$.

It is then easy to calculate the effective mass:

$$M_{\text{eff}} = \frac{M_2 + M_1(1 + K'/K) - K'/\omega^2 - \omega^2 M_1 M_2/K}{1 + x^2 K'/K - \omega^2[x^2 M_1 + (1-x)^2 M_2]/K}. \tag{2.4}$$

M_{eff} is thus frequency dependent, and it also depends on the parameters of the system (M_1, M_2, K, K' and x). To illustrate the idea of negative mass, let us consider the case of an infinitely rigid spring between the two masses ($K \to \infty$). The system is then a $M_1 + M_2$ mass linked to the tube by a spring K', and Eq. (2.4) reduces to $M_{\text{eff}} = (M_1 + M_2) - K'/\omega^2$, which is negative for $\omega^2 < K'/(M_1 + M_2)$. It is interesting to write Newton's second law in this case:

$$-(M_1 + M_2)\omega^2 U + K'U \quad = \quad \Delta P S. \tag{2.5}$$

In response to our forcing pressure, there are two components now: the inertial response, that involves the mass of the system, and the elastic response, which depends on the spring. At low frequency, for $\omega \ll \sqrt{K'/(M_1 + M_2)}$, the elastic force dominates, and we see that $\Delta P > 0$ leads to $U > 0$ this time. The system thus responds in a way that is more natural to our everyday life experience: it moves in the direction of the applied force. However, when analysed from an inertial point of view, it gives an abnormal phase, and a negative mass. A negative mass system is thus merely a system that reacts elastically rather than inertially. Note that this situation is formally analogous to the plasma resonance in electromagnetics, in which the permittivity is negative for frequencies below the plasma resonance [19].

Designing an elementary cell in view of obtaining a negative density consists in including somehow an elastic response that will be interpreted as an abnormal inertial response. The spring K' between the outer ring and the tube is a solution, but it is not the only one. As shown in Fig. 2, Eq. (2.4) can also predict the existence of a regime of negative mass even for $K' = 0$. Here the parameters are $M_1 = 9\,\text{g}$, $M_2 = 1\,\text{g}$, $x = 0.9$, $K = 1000\ \text{N/m}$, and $K' = 0$. We see that the effective mass is negative from about 200 to 600 Hz. Let us look into detail the response of the system as a function of frequency. At low frequency, the two masses move together and we find $M_{\text{eff}} = M_1 + M_2$. For a given frequency, here close to 150 Hz, there is a resonance and the effective mass diverges and becomes negative. We will discuss in section 5 how this resonance frequency depends on the parameters. For now, let us focus on the physical picture. The resonance comes from the different inertial responses of the two masses (because their mass and surface are different), which leads to different displacements U_1 and U_2 and brings the elastic response $K(U_1 - U_2)$ into play, such that the effective mass becomes negative. However as in the case $K' \neq 0$ discussed before, the inertial response dominates the elastic one at higher frequencies, meaning that the effective mass becomes positive again. At high frequency, the asymptotic value of M_{eff} corresponds to two masses in parallel, without connection.

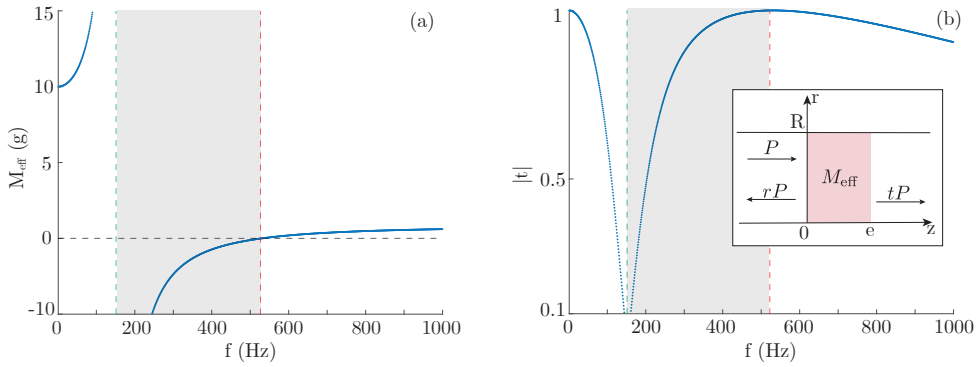

Figure 2. Example of (a) the effective mass and (b) the amplitude of transmission for objects defined by $M_1 = 9\,\text{g}$, $M_2 = 1\,\text{g}$, $x = 0.9$, $K = 10$ kN/m, $K' = 0$ and immersed in a tube filled with air ($k_0 = 2\pi f/c_0$ and $Z0 = \rho_0 c_0$ with $c_0 = 340$ m/s and $\rho_0 = 1.2$ kg.m^{-3}). Inset: sketch of the transmission and the reflection of an incident wave through the effective system.

3. Transmission

In the previous section, we imagined a situation in which we were able to excite the system with a given force ΔPS. In practice, the excitation is rather the result of an incoming wave. Let us consider this more realistic situation. It will also turn out to be a good intermediate calculation for the next section, in which we look at an effective continuous medium. The inset in Fig. 2b shows the situation that we want to calculate: an incident pressure wave $P\exp[\text{i}(k_0 z - \omega t)]$ impinges the object and leads to a reflected wave $rP\exp[\text{i}(-k_0 z - \omega t)]$ and a transmitted one $tP\exp[\text{i}(k_0 z - \omega t)]$, where k_0 is the wavevector for the medium filling the tube (air, for example). Note that we consider only plane waves propagating in the tube. It imposes that the wavelength remains larger than the diameter of the tube, otherwise other modes could be excited, especially when the two parts of the objects exhibit different displacements. For a tube of radius $R = 5\,\text{cm}$ filled with air, the frequency must be lower than 2 kHz.

Let us calculate the coefficients r and t, which will allow us to determine ΔP. The total pressure field on each side of the object can be written (dropping the time dependence)

$$p(z) = P\text{e}^{\text{i}k_0 z} + rP\text{e}^{-\text{i}k_0 z} \quad \text{for } z < 0, \tag{3.1}$$

$$p(z) = tP\text{e}^{\text{i}k_0 z} \quad \text{for } z > e. \tag{3.2}$$

On the other hand, the displacement field is given by

$$u(z) = \frac{\text{i}}{\omega Z_0} P(\text{e}^{\text{i}k_0 z} - r\text{e}^{-\text{i}k_0 z}) \quad \text{for } z < 0, \tag{3.3}$$

$$u(z) = \frac{\text{i}}{\omega Z_0} tP\text{e}^{\text{i}k_0 z} \quad \text{for } z > e, \tag{3.4}$$

where Z_0 is the impedance of the surrounding medium. At this point it is important to introduce a condition on the thickness of the object. We will consider that the wavelengths, in both the host medium and in the constitutive material of the object, are much larger than the thickness e of the object. Hence, we may discard wave propagation in the object, and we can consider that its left and right faces are moving with the same displacement: $u(z = 0) = u(z = e) = U$. It gives a first relationship between r and t:

$$1 - r = t\text{e}^{\text{i}k_0 e}. \tag{3.5}$$

Note that $\exp(\mathrm{i}k_0 e)$ is close to one, but we keep this term because it will be useful in section 4. The second relation is obtained by writing Newton's second law for the object (directly with its effective mass given by Eq. (2.4)):

$$-M_{\text{eff}}\omega^2 U = PS\left(1 + r - t\mathrm{e}^{\mathrm{i}k_0 e}\right). \tag{3.6}$$

Putting Eqs. (3.4)-(3.6) together, we finally obtain:

$$t = \frac{\mathrm{e}^{-\mathrm{i}k_0 e}}{1 + \frac{\omega M_{\text{eff}}}{2\mathrm{i}Z_0 S}}, \tag{3.7}$$

$$r = 1 - t\mathrm{e}^{\mathrm{i}k_0 e}. \tag{3.8}$$

Eq. (3.7) is known as the Mass law, valid for an obstacle that is thinner than the wavelength. It shows that low frequency sound is hard to block, because $|t| \to 1$ for $\omega \to 0$. A high value of surface mass (M_{eff}/S) is necessary for efficiently blocking low frequency noise. This is actually a challenge for metamaterials: having a large effective mass with a light and thin system. Fig. 2b shows the amplitude of the transmission in our example. There is a clear minimum at resonance (when the effective mass diverges) and a maximum when the mass goes through zero.

4. Continuous medium

Now that we know the acoustical behaviour of our elementary cell, we can build a metamaterial. The idea is simply to stack several objects one after the others. For simplicity let us consider that the stacking is periodic, with a distance d from one layer to the other, as illustrated in Fig. 3a. Between the layers, we have the same medium as in the rest of the tube (e.g., air), with k_0 and Z_0. As shown in Appendix A, at the low frequency limit ($k_0 d \ll 1$), the N layers behave as an effective homogeneous liquid of thickness $L = Nd$, with an effective compressibility χ_{eff} and an effective density ρ_{eff} given by

$$\frac{\chi_{\text{eff}}}{\chi_0} = 1 + \frac{\mathrm{i}}{k_0 d}\frac{1 - t - r}{t}, \tag{4.1}$$

$$\frac{\rho_{\text{eff}}}{\rho_0} = 1 + \frac{\mathrm{i}}{k_0 d}\frac{1 - t + r}{t}. \tag{4.2}$$

Inserting the values (3.7) for t and (3.8) for r, we obtain:

$$\chi_{\text{eff}} = \left(1 - \frac{e}{d}\right)\chi_0, \tag{4.3}$$

$$\rho_{\text{eff}} = \left(1 - \frac{e}{d}\right)\rho_0 + \frac{M_{\text{eff}}}{Sd}. \tag{4.4}$$

We can check that these expressions correspond to a mixing law, in which an effective property A_{eff} is given by an average of the properties of its components (A_0, A_1), with a weight corresponding to the volume fraction: $A_{\text{eff}} = (1 - \Phi)A_0 + \Phi A_1$, where Φ is the volume fraction of component 1 in the unit cell. In our case, the volume fraction is given by e/d. The effective compressibility (4.3) is a mixture law with $\chi_1 = 0$, because the inclusion is incompressible (we assumed that both faces of the object had the same displacement). As for Eq. (4.4), it also takes the form of a mixture law if we define a density $\rho_1 = M_{\text{eff}}/(Se)$ for the inclusion.

The multilayer has thus the same qualitative behaviour as its constitutive elements, as shown in Fig. 3b, with a resonance followed by a regime of negative density.

5. Frequency range of negative mass given by the toy model

We now study in more details the predictions of the toy model. We take advantage of its simplicity to derive analytical predictions for the frequency ranges where the effective mass is negative (henceforth called "negative bands" for simplicity), and which sets of parameters maximise these

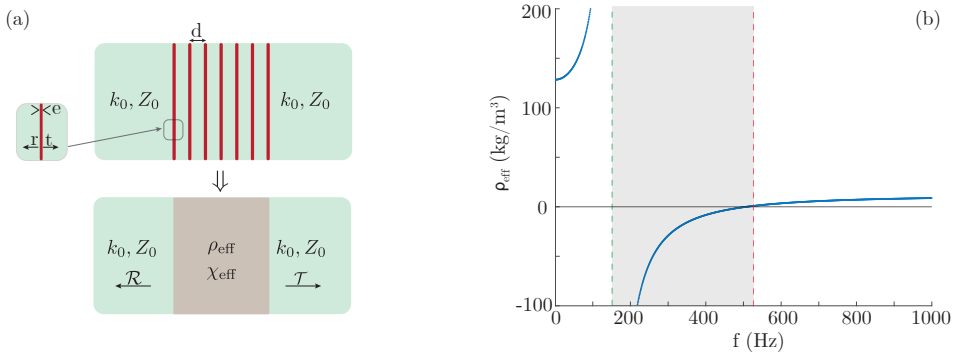

Figure 3. (a) A succession of layers, characterised by their transmission and reflection coefficients (t,r) is equivalent, at low frequency, to a homogeneous medium with an effective compressibility χ_{eff} and an effective density ρ_{eff}, given by Eqs. (4.1) and (4.2). (b) Effective density for a multilayer made of an elementary cell as in Fig. 2 ($M_1 = 9$ g, $M_2 = 1$ g, $x = 0.9$, $K = 10$ kN/m, $K' = 0$), for $e = 1$ mm and $d = 10$ mm.

ranges. Since we saw that ρ_{eff} was an affine function of M_{eff} (eq. (4.4)), all our conclusions on the effective mass will also apply on the negative density, provided the density of the host medium is low (as for air). In order to explore the conditions for a negative effective mass, we introduce four dimensionless parameters describing our system:

$$x = \frac{S_2}{S_1 + S_2}, \tag{5.1}$$

$$\mu = \frac{M_2}{M_1 + M_2}, \tag{5.2}$$

$$\kappa = \frac{K'}{K}, \tag{5.3}$$

$$\Omega^2 = \frac{M_1 + M_2}{K}\omega^2, \tag{5.4}$$

with x the surface fraction occupied by the central cylinder (already introduced in Sec. 2), μ the mass fraction carried by the central mass, κ the ratio between the stiffness of the two springs and Ω a dimensionless frequency. Using these dimensionless parameters on can rewrite eq. (2.4) as:

$$m_{\text{eff}} \equiv \frac{M_{\text{eff}}}{M_1 + M_2} = \frac{\mu + (1-\mu)(1+\kappa) - \kappa/\Omega^2 - \mu(1-\mu)\Omega^2}{1 + x^2\kappa - [(1-\mu)x^2 + \mu(1-x)^2]\Omega^2}, \tag{5.5}$$

where m_{eff} is the dimensionless effective mass.

(a) Case $K' = 0$

First, let us look at the simple case where $\kappa = 0$. The dimensionless effective mass becomes

$$m_{\text{eff}} = \frac{1 - \mu(1-\mu)\Omega^2}{1 - [(1-\mu)x^2 + \mu(1-x)^2]\Omega^2}. \tag{5.6}$$

In Fig. 4a we plot the dimensionless effective mass of Fig. 2a as a function of the dimensionless frequency.

At low frequency, as previously explained, the two masses move in block:

$$\lim_{\Omega \to 0} m_{\text{eff}} \equiv 1. \tag{5.7}$$

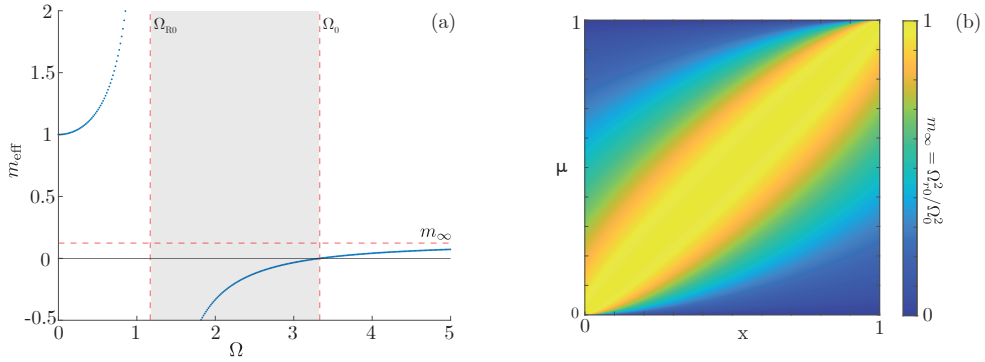

Figure 4. Case $\kappa = 0$. (a) Dimensionless effective mass as a function of the dimensionless frequency Ω for $\mu = 0.1$ and $x = 0.9$. (b) Ratio between the two bounds of the negative band as function of the surface fraction occupied by the central cylinder x and the mass fraction carried by the central mass μ. The smaller the ratio, the larger the negative band.

Moreover, Eq. (5.6) shows immediately that the effective mass cancels out for one characteristic frequency, Ω_0, and presents one frequency resonance Ω_{r0}:

$$\Omega_0^2 = \frac{1}{\mu(1-\mu)}, \tag{5.8}$$

$$\Omega_{r0}^2 = \frac{1}{(1-\mu)x^2 + \mu(1-x)^2}. \tag{5.9}$$

Finally, at high frequency, the effective mass does not depend on the stiffness of the spring between the two masses. It takes the form of two masses in parallel:

$$\lim_{\Omega\to\infty} m_{\text{eff}} \equiv m_{\infty} = \left[\frac{x^2}{\mu} + \frac{(1-x)^2}{1-\mu}\right]^{-1}. \tag{5.10}$$

As illustrated in Fig. 4a, the effective mass is negative between Ω_{r0} and Ω_0. To appreciate the width of the negative band, we study Ω_{r0}/Ω_0, which will be small for a large negative band. Interestingly, this ratio is equal to the high frequency limit of the effective mass, and it is almost symetrical in x and μ:

$$\frac{\Omega_{r0}^2}{\Omega_0^2} = m_{\infty} = \left[1 + \frac{(x-\mu)^2}{\mu(1-\mu)}\right]^{-1}. \tag{5.11}$$

Fig. 4b proposes a visualisation of how $(\Omega_{r0}/\Omega_0)^2$ depends on x and μ. The symmetry is visible, and one can conclude that a large negative band can be obtained either with a small μ and a large x, or with the opposite, a small x and a large μ. We will see in Section 7 that both cases have been explored in experimental systems.

(b) Case $K' \neq 0$

Let us now consider the effect of the spring between the tube and the annulus. Since the analysis is more involved than in the previous subsection, most calculations are deferred to Appendix B. The behaviour of the effective mass is now much richer, as exemplified in Fig. 5.

From eq. (5.5), at low frequency, on can get a first expression:

$$\lim_{\Omega\to 0} m_{\text{eff}} = -\frac{\kappa}{(1+x^2\kappa)\Omega^2}, \tag{5.12}$$

In this limit the effective mass is no longer the sum of the two masses. The negative sign of the limit (5.12) shows that the elastic response conferred by the spring of stiffness K' dominates

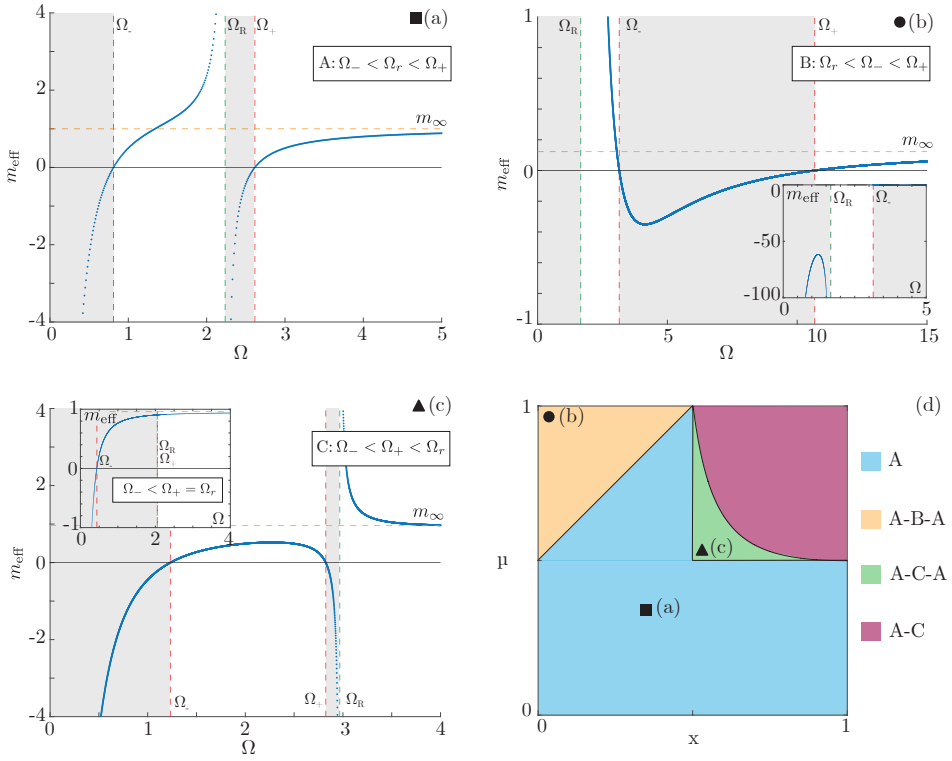

Figure 5. Plots of the effective mass as a function of frequency, showing the three different qualitative behaviours depending on the position of the resonance frequency Ω_r respective to $\Omega_\pm$: (a) case $\Omega_- < \Omega_r < \Omega_+$; (b) case $\Omega_r < \Omega_- < \Omega_+$; (c) case $\Omega_- < \Omega_+ < \Omega_r$. The values of the parameters chosen to plot these graphs are: (a) $x = 1/3$, $\mu = 1/3$, $\kappa = 1$; (b) $x = 0.1$, $\mu = 0.9$, $\kappa = 101.4$; (c) $x = 0.65$, $\mu = 0.55$, $\kappa = 3$. The inset of (c) shows a degenerate case where $\Omega_r = \Omega_+$ [values of the parameters: Inset:$\kappa = \kappa_- = 0.2$ (d) $x = 0.65$, $\mu = 0.55$, $\kappa = \kappa_- = 0.2$, where κ_- is defined by (B 6)]. (d) Diagram showing which of the three cases occur as κ varies at given values of x and μ. In blue, case (a) $\Omega_- < \Omega_r < \Omega_+$ happens whatever κ. In orange, as κ increases, there is a first transition from (a) to case (b) $\Omega_r < \Omega_- < \Omega_+$, and a second one back to (a). In green, as κ increases, there is a first transition from (a) to case (c) $\Omega_- < \Omega_+ < \Omega_r$, and a second one back to (a). In red, as κ increases, there is a single transition from (a) to (c). The three symbols ■, ● and ▲ in panel d indicate the values of x and μ corresponding to the plots in panels a, b and c, respectively.

the behaviour of the system at low frequency. This is essentially different from the limit (5.7), taken from a case where the stiffness K' is absent, and where elastic effects dominate only at intermediate frequency, as the two masses start moving at different amplitudes and phases.

In contrast, at high frequency, the effective mass remains independent of the two stiffnesses. With or without springs the effective mass remains the same quantity, given by (5.10):

$$\lim_{\Omega \to \infty} m_{\text{eff}} \equiv m_\infty \tag{5.13}$$

To study the frequency dependence of the effective mass, we can recast (5.5) as:

$$m_{\text{eff}} = -\frac{\kappa}{(1 + x^2\kappa)\Omega^2} \frac{(1 - \Omega^2/\Omega_-^2)(1 - \Omega^2/\Omega_+^2)}{(1 - \Omega^2/\Omega_r^2)}, \tag{5.14}$$

which shows that the effective mass now cancels for two characteristic frequencies $\Omega_\pm$, and that one frequency resonance Ω_r still appears:

$$\Omega_\pm^2 = \frac{1}{2\mu(1-\mu)}\left\{\mu + (1-\mu)(1+\kappa) \pm \sqrt{[\mu-(1-\mu)\kappa]^2 + (1-\mu)[1+\mu+2(1-\mu)\kappa]}\right\}, \tag{5.15}$$

and:

$$\Omega_r^2 = (1+x^2\kappa)\Omega_{r0}^2. \tag{5.16}$$

The factorised expression (5.14) shows that one can expect three changes of sign for the effective mass, hence two negative bands. If the three frequencies Ω_-, Ω_+ and Ω_r are ordered as: $\Omega_1 < \Omega_2 < \Omega_3$, the two negative bands appear at frequencies below Ω_1, and between frequencies Ω_2 and Ω_3.

Since $\Omega_- < \Omega_+$ from their definition (5.15), we must compare Ω_r to the two frequencies $\Omega_\pm$ to determine the bounds of the negative bands in terms of these three frequencies. Three cases are possible: (a) $\Omega_- < \Omega_r < \Omega_+$, where one negative band is below Ω_-, and one between Ω_r and Ω_+ (Fig. 5a); (b) $\Omega_r < \Omega_- < \Omega_+$, where one negative band is below Ω_r, and one between Ω_- and Ω_+ (Fig. 5b); (c) $\Omega_- < \Omega_+ < \Omega_r$, where one negative band is below Ω_-, and one between Ω_+ and Ω_r (Fig. 5c). Moreover, degenerate cases are possible when $\Omega_r = \Omega_-$ or $\Omega_r = \Omega_+$. Then (5.14) shows that both the resonance and the second negative band vanish, and that a single low-frequency band remains present; this degenerate case is illustrated in the inset of Fig. 5c.

Now that the different cases (a), (b) and (c) have been presented, we must predict in which range of parameters (x, μ, κ) they are found. First, it is worth noting from (5.15) and (5.16) that $\lim_{\kappa\to 0}\Omega_- = 0$, while $\lim_{\kappa\to 0}\Omega_r = \Omega_{r0} > 0$ and $\lim_{\kappa\to 0}\Omega_+ = \Omega_0 > \Omega_{r0}$ where Ω_0 and Ω_{r0} are given by (5.8) and (5.9), hence the condition (a) $\Omega_- < \Omega_r < \Omega_+$ is fulfilled for sufficiently low values of κ, whatever x and μ. Hence, for any fixed couple of values (x, μ), we study whether the ordering changes as κ varies between 0 and ∞. The result of such a study is summarised in Fig. 5d (more details are given in Appendix B), where in the blue region the condition (a) is met whatever the value of κ, while in the other regions, varying κ for fixed x and μ results in changes of ordering of Ω_r relative to $\Omega_\pm$.

6. Dissipation

We now consider the effect of dissipation. For simplicity, we restrict ourselves to adding an imaginary part to the stiffness $K = K_r + \mathrm{i}\, K_i$, as if there were a dashpot between the two moving masses.

In the simplest case $K' = 0$, the effective mass is given by $m_{\text{eff}} = m_r + \mathrm{i}\, m_i$ with:

$$m_r = \frac{(1-\Omega^2/\Omega_0^2)(1-\Omega^2/\Omega_{r0}^2)+\alpha^2}{(1-\Omega^2/\Omega_{r0}^2)^2+\alpha^2}, \tag{6.1}$$

$$m_i = \alpha\left(\frac{1}{\Omega_{r0}^2} - \frac{1}{\Omega_0^2}\right)\frac{\Omega^2}{(1-\Omega^2/\Omega_{r0}^2)^2+\alpha^2}, \tag{6.2}$$

where the dimensionless parameter α is the ratio between the imaginary part and the real part of the complex stiffness :

$$\alpha \equiv \frac{K_i}{K_r}. \tag{6.3}$$

Figure 6a shows how the system considered in figure 4 is modified by taking dissipation into account. The negative band is reduced by the presence of dissipation. As expected for a resonance, the imaginary part presents a maximum around the frequency resonance decreasing with α. Interestingly, the frequency of this maximum slightly increases with α ($\Omega_c^2 = \Omega_{r0}^2\sqrt{1+\alpha^2}$). The effective mass cancels for two frequencies $\Omega_{\alpha\pm}$ up to a critical value of α. From the numerator of

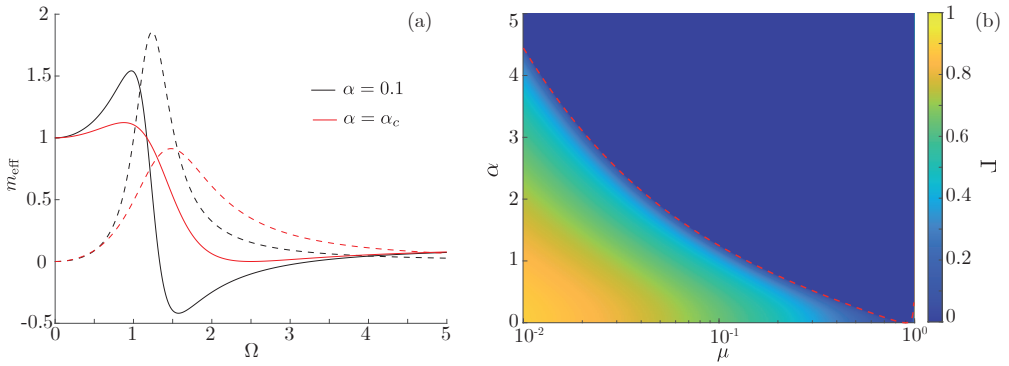

Figure 6. Influence of the dissipation for $\kappa = 0$. (a) Real part (continuous lines) and imaginary part (dash lines) for the same case as in Fig. 4 ($x = 0.1$, $\mu = 0.9$), but with dissipation, for two different values of α: $\alpha = 0.1$ (black lines) and $\alpha = \alpha_c$ (red lines). (b) Width of the negative frequency band $\Gamma = (\Omega_{\alpha+} - \Omega_{\alpha-})/\Omega_{\alpha+}$ (where $\Omega_{\alpha\pm}$ are the zero-mass frequencies) for $x = 0.9$. The red dashed line indicates the extinction of the negative frequency band (Eq. (6.4)).

.

Eq. (6.1), one gets that the negative band vanishes for:

$$\alpha_c = \frac{1}{2}\left(\frac{\Omega_0}{\Omega_{r0}} - \frac{\Omega_{r0}}{\Omega_0}\right), \tag{6.4}$$

The width of the negative frequency band is quantified by $\Gamma = (\Omega_{\alpha+} - \Omega_{\alpha-})/\Omega_{\alpha+}$. This quantity Γ is represented in Fig. 6b for a fixed value of x.

In the general case where both stiffnesses K and K' are present, it is easy to show that the main effect of dissipation is to suppress the second negative band (see Sec. 5(b)) for a large enough value of α. The proof is presented in Appendix C; however, there is no analytical prediction of α_c, contrary to Eq. (6.4) in the case $\kappa = 0$.

7. Comparison with real systems

Despite its crudeness, the toy model that we propose can reproduce, at least qualitatively, the acoustic behaviours reported in some experimental systems. We will discuss three types of systems.

A first example is the negative density obtained by placing a series of membranes [3,9] in a tube. Each elastic membrane, attached to the tube, confers a stiffness K' to the system, and has a mass M_1, leading to a plasma-like resonance, as discussed in [19], below which the effective density is negative.

Two other examples associate a membrane and a heavier structure: the decorated membrane resonators (DMR), and the liquid foams. Interestingly, each case illustrates one of the two favourable configurations which we identified for the emergence of a negative band: a heavy central part with a limited surface (large μ and small x) or a light one with a large surface (small μ and large x).

(a) Membranes

Due to its ability to bring an elastic response to the system, a membrane is a good candidate for obtaining a negative effective density. One of the first experimental evidences of a negative density was brought by Lee *et al.* [3] who placed a series of membranes in a tube and demonstrated the existence of a negative density below a critical frequency f_c. Figure 7a shows the phase

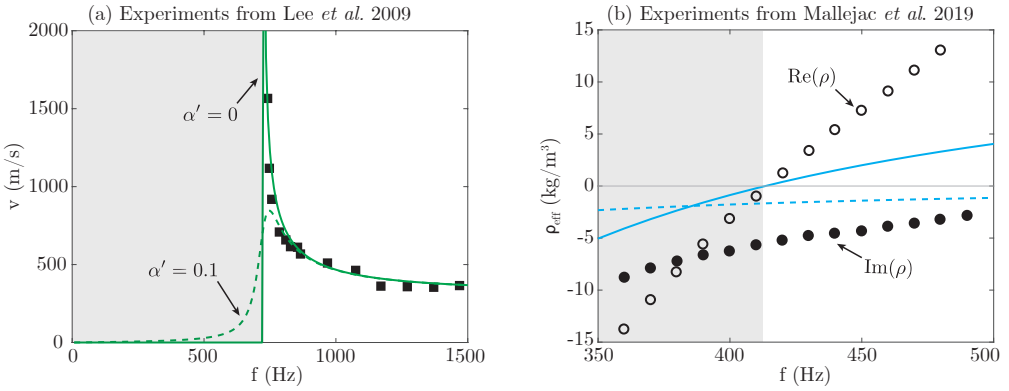

Figure 7. Comparison between experimental results obtained with membranes and the toy model. (a) Phase velocity as a function of frequency for a series of $10\,\mu$m-thick membranes separated by $d = 7$ cm in a 3.2 cm-radius tube (Fig. 5 of Ref. [3] — black square). With $M = 30$ mg and $K' = 6210$ N/m, the toy model gives a good agreement (solid green line). Adding dissipation (dashed green line) lowers the velocity peak. (b) Effective density for $102\,\mu$m-thick plates separated by $d = 1$ cm in a 1.5 cm-radius tube (Fig. 4 of Ref. [9] — white circle for the real part and black circle for the imaginary). The toy model prediction is plotted for $M = 101$ mg, $K' = 738$ N/m, and a dissipation of $\alpha' = 0.13$ (solid blue line for the real part and dashed blue line for the imaginary).

velocity v that they measured in their system, as a function of frequency. As $v = (\rho\chi)^{-1/2}$, the passage through $\rho = 0$ is associated to a peak in velocity. Injecting eq. (2.4) into eq. (4.4) for $K \to \infty$, we obtain the following law for the effective density of the system:

$$\rho_{\text{eff}} = \left(1 - \frac{e}{d}\right)\rho_g + \frac{M - K'/\omega^2}{Sd} \tag{7.1}$$

$$= \rho'\left(1 - \frac{\omega_c^2}{\omega^2}\right), \tag{7.2}$$

with $\rho' = (1 - e/d)\rho_g + \rho_m e/d$ and $\omega_c^2 = K'/(Sd\rho')$ (ρ_g is the density of the gas, and ρ_m that of the membrane). The experimental system was made with thin membranes ($e = 10\,\mu$m, $\rho_m = 940\,\text{kg/m}^3$) in a $R = 1.5$ cm tube, with a separation of $d = 7$ cm. We can thus evaluate $\rho' = 1.34\,\text{kg/m}^3$. For K', we adjust its value to match the cutoff frequency $f_c = 720$ Hz, which leads to $K' = 6210$ N/m. As shown in Fig. 7a, with these values of the parameters, the measured velocity is well captured by the toy model.

Metamaterials with density close to zero have attracted attention recently because they could open the way to narrow and long channels capable of efficiently coupling wave guides [8]. Within this perspective, a recent study by Malléjac *et al.* [9] has conducted careful experiments on a system of thin plates in a tube. The measured effective density is reproduced in Fig. 7b, the open symbols showing the real part of the density, and the black ones the imaginary. The data were obtained with plates ($e = 102\,\mu$m, $\rho_m = 1400\,\text{kg/m}^3$) with a spacing of $d = 1$ cm in a 1.5 cm tube. The material of the plates was characterized by a Young modulus of $E = E_0(1 + \mathrm{i}\beta)$, with $E_0 = 4.6$ GPa and $\beta = 0.13$, and a Poisson ratio of 0.4.

Adapting the toy model to the mass of the plates and the geometry of the system, we take a total mass $M = 101$ mg, which leads to $\rho' = 15.5\,\text{kg/m}^3$. For the spring, we select the value that leads to the correct cutoff frequency of 413 Hz: $K' = 748$ N/m. And we add an imaginary part of $\alpha' = 13\%$ to account for the dissipation. The prediction of the toy model with these parameters is shown in Fig. 7b. As in the experiments, it suggests that the imaginary part of the density is not negligible. It fails, however, at reproducing the correct trend for the increase of density with frequency. This suggests that the toy model, which has only one degree of freedom, cannot capture

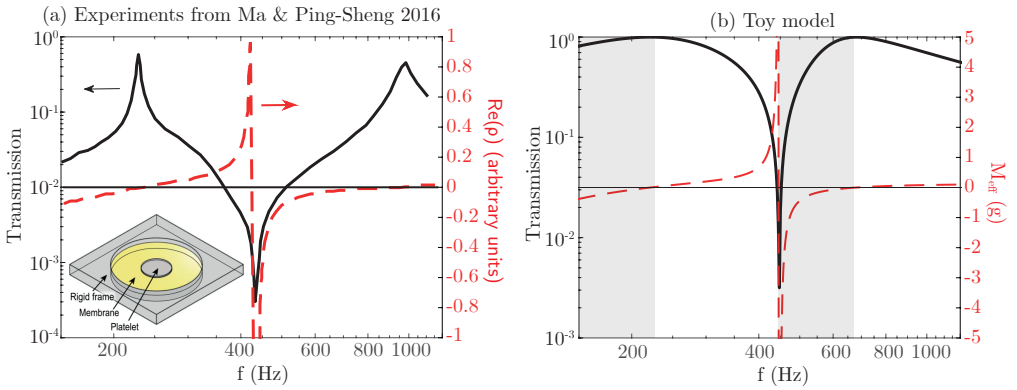

Figure 8. Comparison between experimental results obtained with a decorated membrane [14] (a) and our toy model (b). Both panels show the transmission (black curves) and the effective mass (red dashed curves) as function of frequency. The inset is a drawing of the experimental setup. Data and drawing on the left panels are extracted from figure 3 in the review by Ma and Ping-Sheng [2]. For the toy model, we plot Eq. (2.4) for parameters $M_1 + M_2 = 277\,\text{mg}$, $K = 1.1\,\text{kN/m}$, $x = 0.1$, $\mu = 0.62$, and $\kappa = 0.53$.

the whole behaviour of the plates. The interest of the toy model in this case is limited to its ability to reproduce qualitatively the observed phenomenon.

(b) Decorated membrane resonators

Loading a membrane with a heavier element leads to what is often called a decorated membrane resonator (DMR). A typical example is shown in the inset of figure 8: a latex membrane (in yellow) is stretched on a rigid frame, and loaded with a plastic disk (in grey). Figure 8a is extracted from reference [14] and shows the experimental transmission as a function of frequency, obtained with such a system (black line). Two peaks are visible, with a very low minimum of transmission in between. These features can be interpreted in terms of an effective mass (red dashed curve), which goes through zero for the peaks of transmission, and increases abruptly at the resonance, corresponding to the minimum of transmission.

We see that the effective density of this system is very similar to what was obtained in figure 2a for our toy model. It is tempting to go a step further and look if we can obtain a quantitative comparison. The membrane is 0.2 mm thick, with a density of $980\,\text{kg/m}^3$ and a radius of 14 mm. The disk has a weight of 125 mg and a radius of 14 mm [20]. Identifying the disk (and the part of membrane beneath) with mass M_2 in the toy model, we obtain $M_2 = 173\,\text{mg}$ and $M_1 = 104\,\text{mg}$, which corresponds to $\mu = 0.62$. The geometry leads to $x = 0.1$. Chosing K and K' is less straightforward because the elasticity of a membrane cannot be reduced to a simple set of two springs. By tuning the parameters, we found that $K = 1.1\,\text{kN/m}$ and $\kappa = 0.53$ lead to the effective mass shown in figure 8b (dashed red plot). Comparison with the experimental results is qualitatively good, with the same range of frequencies of the two negative regimes. However, note that the density is in arbitrary units in figure 8a, meaning that we cannot quantitavely compare the agreement. We can do it with the transmission coefficient (black line), and it turns out to be quite different from the experimental one, with less sharp peaks and minimum. As in Fig 7b, it probably comes from the fact that the real membrane has a much richer dynamics than what can be simulated with one mass and two springs. Despite this lack of quantitative agreement, the toy model seems to capture some of the physical effects at play in the real system. It might be interesting for helping in designing new DMR, guided by an analytical expression.

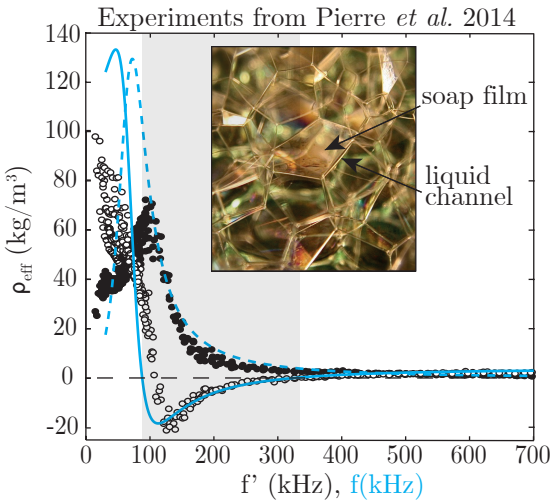

Figure 9. Comparison between experimental results obtained with a liquid foam and the toy-model. The real and imaginary parts of the effective density are shown as functions of the frequency (rescaled frequency f' for the experiments, see text for details). The inset is a photograph of a liquid foam, showing the distribution of the liquid in two different structures: the films and the channels. Data are extracted from figure 5 in our previous article [17]. For the toy model, we plot Eq. (2.4) for parameters $M_1 + M_2 = 3 \times 10^{-11}$ kg, $K = 180$ mN/m, $x = 0.2$, $\mu = 0.001$ and $\alpha = 1$.

(c) Liquid foams

Liquid foams are made of such a high volume fraction of gas that the bubbles are not spherical anymore and adopt polyhedral shapes, as illustrated in the inset of figure 9. The liquid is then contained in two different structures: the channels and the films. In 2014, we reported experimental evidence that the acoustic density of a liquid foam could be negative. Figure 9 shows an experimental result, adapted from [17], with the real (white symbols) and imaginary (black symbols) parts of the density as functions of frequency. The foams had a liquid volume fraction of $\Phi_\ell = 11\%$ and a bubble median radius of $R_0 = 40\,\mu$m. We proved that this negative band was found at any other median radius R, provided a rescaled frequency $f' = f(R/R_0)^{1.5}$ was used (see [17] for details).

We see in Figure 9 that the real part of the density (open symbols) takes negative values between 100 and 400 kHz. This figure is strikingly similar to figure 6a, which corresponds to the toy model in the $K' = 0$ case. At first sight, this case of the toy model seems far from a real situation, because it consists in considering a mass that can slide without friction in a tube. But the very particular structure of the liquid foam leads to a behaviour that is similar to this idealised situation. When an acoustic wave propagates through the liquid foam, it encounters soap films and liquid channels. Most of the liquid is in the channels, the films being very thin elements. The films carry the elastic response, due to their surface tension. In total, the acoustic behaviour of the foam can thus be modelled as an heavy mass (the liquid channels) around a light one of large relative surface (the films) with a restoring force.

Let us see if we can determine the parameters of the toy model that will reproduce the measurements reported in figure 9. Equation (4.4) for the effective density can be rewritten as a function of the liquid volume fraction:

$$\rho_{\text{eff}} = (1 - \Phi_\ell)\rho_g + \Phi_\ell \frac{M_{\text{eff}}}{Se} = (1 - \Phi_\ell)\rho_g + \Phi_\ell \rho_\ell m_{\text{eff}}. \tag{7.3}$$

To calculate m_{eff}, the values of $M_1 + M_2$, $K(1 + \mathrm{i}\alpha)$, x and μ are required. The surface fraction occupied by soap films in a liquid foam has been studied by Princen [21]. It depends on the liquid fraction, and for $\Phi_\ell = 11\%$, one finds that $x = 0.2$. The total mass $M_1 + M_2$ can be estimated by looking at the mass of a unit cell, whose volume is given by the median radius of the bubbles in the foam: $M_1 + M_2 = \Phi_\ell \times \frac{4}{3} R_0^3 \rho_\ell$. We find a mass of the order of 3×10^{-11} kg. The other parameters are tuned to recover the same frequencies for the beginning and the end of the negative regime, and we obtain $K = 0.18\,\mathrm{N/m}$, $\alpha = 1$ and $\mu = 10^{-3}$. Figure 9 shows the complex effective density given by the toy model for this set of parameters. We see that it compares well to the experimental results, even quantitatively to a certain extent: we obtain good orders of magnitude for the real and imaginary parts of the density. Note that the level of dissipation is far from being negligible ($\alpha = 1$). According to our analytical study of the model, the negative band survives to this dissipation because parameter μ is particularly low (see figure 6b).

Liquid foams appear as quite unusual acoustic metamaterials because they combine several characteristics that are in principle not favourable to the emergence of a negative band: they are polydisperse, disordered, and highly dissipative. The negative band is robust because foams are intrinsically constituted of large but light elements (the films) elastically attached to small but massive elements (the liquid channels).

8. Conclusion

In this article, we have introduced a simple toy model, constituted at most of two masses, two springs and one dissipative item, to clarify the occurrence of negative effective density in acoustic metamaterials. We have shown three different sets of results. (i) We have made explicit how to derive a transmission coefficient from the single unit of the toy model, and how, when coupled to the ambient medium, its behaviour can be modelled at the macroscopic level as an effective continuous medium. (ii) With a detailed study of the toy model, we have clarified for which frequency range a negative mass can be expected. (iii) We have compared our predictions to real experimental metamaterials and found a good agreement, at least qualitatively.

Beyond its didactic interest, this toy model might be a useful tool to design acoustic metamatarials. Note that it could be generalised to systems with resonances in density and compressibility, by adding masses in series. More complex systems could then be modelled, such as the double DMR [13], or the "acoustic sandwiches" [22].

Acknowledgements. We acknowledge invaluable discussions with the participants of the ANR project Samousse.

References

1. Pendry J. 2006. Metamaterials in the sunshine. *Nature Materials* **5**
2. Ma G. and Sheng P. 2016. Acoustic metamaterials: From local resonances to broad horizons. *Science Advance* **2**.
3. Lee SH, Park CM, Seo YM, Wang ZG, Kim CK 2009 Acoustic metamaterial with negative density. *Phys. Lett. A* **373**, 4464–4469.
4. Park CM, Park JJ, Lee SH, Seo YM, Kim CK, Lee SH 2011 Amplification of acoustic evanescent waves using metamaterial slabs. *Phys. Rev. Lett.* **107**, 194301.
5. Varansi S. *et al.* 2013. The low frequency performance of metamaterial barriers based on cellular structures. *Applied Physics* **74**
6. Duan Y, Luo J, Wang G, Hang ZH, Hou B, Li J, Sheng P, Lai Y 2015 Theoretical requirements for broadband perfect absorption of acoustic waves by ultra-thin elastic meta-films. *Sci. Rep.* **5**, 12139.
7. Lee S.H. *et al.* 2010. Composite Acoustic Medium with Simultaneously Negative Density and Modulus. *Physical Review Letters* **104**
8. Fleury R. and Alu. 2013. Extraordinary Sound Transmission through Density-Near-Zero Ultranarrow Channels. *Physical Review Letters* **111**
9. Mallejac *et al.* 2019. Zero-phase propagation in realistic plate- type acoustic metamaterials. *Applied Physics Letters* **115**
10. Mallejac *et al.* 2020. Doping of a plate-type acoustic metamaterial *Physical Review B* **102**

11. Mallejac *et al.* 2021. Experimental evidence of a hiding zone in a density-near-zero acoustic metamaterial *Journal of Applied Physics* **129**
12. Yang Z. *et al.* 2008. Membrane-Type Acoustic Metamaterial with Negative Dynamic Mass. *Physical Review Letters* **101**
13. Yang et al, 2013, Coupled Membranes with Doubly Negative Mass Density and Bulk Modulus. *Physical Review Letters* **110**
14. Ma G. *et al.* 2014. Acoustic metasurface with hybrid resonances. *Nature Materials* **13**
15. Bongard F. *et al.* 2010. Acoustic transmission line metamaterial with negative/zero/positive refractive index. *Physical Review B* **82**.
16. Roca D. and Hussein M. I. 2021. Broadband and intense sound transmission loss by a coupled-resonance acoustic metamaterial, *Arxiv*.
17. Pierre J. *et al.* 2014. Resonant Acoustic Propagation and Negative Density in Liquid Foams. *Physical Review Letters* **112**
18. Wood A. B. 1941. *A text book of sound*,G. Bell and Sons, London
19. Jackson, J. D. (1999). Classical electrodynamics.
20. G. Ma G. 2012 *Membrane-type acoustic metamaterials*, Thesis (Ph.D.), Hong Kong University of Science and Technology
21. Princen H. M. 1985. Rheology of foams and highly concentrated emulsions. II. Experimental study of the yield stress and wall effects for concentrated oil-in-water emulsions. *J. Colloid Interface Sci.* **105**
22. Bolton J.S. *et al.* 1996. Sound transmission through multi-Panel structures lined with elastic porous materials *Journal of Sound and Vibration* **191**.
23. Brekhovskikh L. M. 1980. *Waves in Layered Media*, 2nd Ed., Academic Press.

A. Effective medium

In this Appendix we show that N layers characterised by their transmission and reflection coefficients (t, r) are equivalent, at low frequency, to a homogeneous medium with effective compressibility and density. The idea is to demonstrate that the N-layer system gives the same total reflection and transmission coefficients, $\mathcal{R}$ and $\mathcal{T}$, as an effective medium. Let us consider (see Fig. 3a) a homogeneous medium of thickness $L = Nd$, with wavenumber k and impedance Z. The total reflection and transmission coefficients are given by:

$$\mathcal{R} = y\left[1-(1-y^2)\frac{\mathrm{e}^{2\mathrm{i}kL}}{1-y^2\mathrm{e}^{2\mathrm{i}kL}}\right], \tag{A 1}$$

$$\mathcal{T} = (1-y^2)\frac{\mathrm{e}^{\mathrm{i}kL}}{1-y^2\mathrm{e}^{2\mathrm{i}kL}}, \tag{A 2}$$

where $y = (Z - Z_0)/(Z + Z_0)$. We want to show that the transmission and reflection coefficients through the multi-layer system can be written in the same form, with Z and k being effective quantities that can be expressed as functions of r and t.

Instead of handling Eq. (A 1), we will consider the ratio:

$$\mathcal{R}/\mathcal{T} = \frac{y}{1-y^2}\left(\mathrm{e}^{-\mathrm{i}kL}-\mathrm{e}^{\mathrm{i}kL}\right). \tag{A 3}$$

We will show that the multi-layer system can satisfy (A 2) and (A 3) if k and y are related to r and t by

$$\frac{r}{t} = \frac{y}{1-y^2}\left(\mathrm{e}^{-\mathrm{i}kd}-\mathrm{e}^{\mathrm{i}kd}\right), \tag{A 4}$$

$$\frac{1}{t} = \frac{\mathrm{e}^{\mathrm{i}k_0 d}}{1-y^2}\left(\mathrm{e}^{-\mathrm{i}kd}-y^2\mathrm{e}^{\mathrm{i}kd}\right). \tag{A 5}$$

We follow a recursive sequence. For the initialisation ($N = 1$), we consider one object with a thickness d of the host medium around it. We then obtain

$$\mathcal{R}_1 = r\mathrm{e}^{\mathrm{i}k_0 d}, \tag{A 6}$$

$$\mathcal{T}_1 = t\mathrm{e}^{\mathrm{i}k_0 d}, \tag{A 7}$$

which satisfy conditions (A 2) and (A 3) if k and y verify (A 4) and (A 5), with $L = d$.

For the recursivity, we want to show that if $\mathcal{T}_N$ verifies (A 2) and $\mathcal{R}_N/\mathcal{T}_N$ verifies (A 3), then $\mathcal{T}_{N+1}$ and $\mathcal{R}_{N+1}/\mathcal{T}_{N+1}$ also do. Going from N to $N+1$ layers is simply done by a multiple reflection calculation, adding the extra layer on the left. We obtain [23]

$$\mathcal{R}_{N+1} = r\mathrm{e}^{\mathrm{i}k_0 d} + \mathrm{e}^{\mathrm{i}k_0 d}\frac{t^2\mathcal{R}_N\mathrm{e}^{\mathrm{i}k_0 d}}{1 - r\mathcal{R}_N\mathrm{e}^{\mathrm{i}k_0 d}}, \tag{A 8a}$$

$$\mathcal{T}_{N+1} = \frac{\mathcal{T}_N t\mathrm{e}^{\mathrm{i}k_0 d}}{1 - r\mathcal{R}_N\mathrm{e}^{\mathrm{i}k_0 d}}, \tag{A 8b}$$

which leads to

$$\frac{1}{\mathcal{T}_{N+1}} = \frac{1}{t\mathcal{T}_N\mathrm{e}^{\mathrm{i}k_0 d}} - \frac{r\mathcal{R}_N}{t\mathcal{T}_N}, \tag{A 9a}$$

$$\frac{\mathcal{R}_{N+1}}{\mathcal{T}_{N+1}} = \frac{r}{t\mathcal{T}_N} + \left(t - \frac{r^2}{t}\right)\mathrm{e}^{\mathrm{i}k_0 d}\frac{\mathcal{R}_N}{\mathcal{T}_N}. \tag{A 9b}$$

It can be checked that when (A 4) and (A 5) are injected into those equations, we obtain

$$\frac{1}{\mathcal{T}_{N+1}} = \frac{1}{1-y^2}\left[\mathrm{e}^{-\mathrm{i}k(N+1)d} - y^2\mathrm{e}^{\mathrm{i}k(N+1)d}\right] \tag{A 10a}$$

$$\frac{\mathcal{R}_{N+1}}{\mathcal{T}_{N+1}} = \frac{y}{1-y^2}\left[\mathrm{e}^{-\mathrm{i}k(N+1)d} - \mathrm{e}^{\mathrm{i}k(N+1)d}\right], \tag{A 10b}$$

as expected.

From equations (A 4) and (A 5), we can calculate k and Z as functions of r and t. We will only consider the large-wavelength case, for which $k_0 d \ll 1$ and $kd \ll 1$. The calculations are easier when using ρ and χ instead of k and Z, using the following relationships:

$$k\frac{x}{1-x^2} = \frac{k_0}{4}\left(\frac{\rho}{\rho_0} - \frac{\chi}{\chi_0}\right), \tag{A 11}$$

$$k\frac{1+x^2}{1-x^2} = \frac{k_0}{2}\left(\frac{\rho}{\rho_0} + \frac{\chi}{\chi_0}\right), \tag{A 12}$$

and we finally obtain equations (4.1) and (4.2):

$$\frac{\chi_{\mathrm{eff}}}{\chi_0} = 1 + \frac{\mathrm{i}}{k_0 d}\frac{1-t-r}{t}, \tag{A 13a}$$

$$\frac{\rho_{\mathrm{eff}}}{\rho_0} = 1 + \frac{\mathrm{i}}{k_0 d}\frac{1-t+r}{t}. \tag{A 13b}$$

Interestingly, we find that if $t = 1 + r$, only the compressibility is affected by the layers, while if $t = 1 - r$, only the density is. This is analogous to the case of three-dimensional inclusions, whose monopolar response affects the compressibility, and dipolar one the density.

B. Details about how diagram of Fig 5d is obtained

In this section we present some details to determine the position of frequency resonance Ω_r comparatively to zero-mass frequencies $\Omega_\pm$. The relation depends on the stiffness ratio κ for a fixed couple $(x, \mu) \in E = [0,1]^2$.

We must solve the equation $\Omega_\pm^2 = \Omega_r^2$. From Eqs. (5.15) and (5.16), it is equivalent to:

$$[\mu - (1-\mu)\kappa]^2 + (1-\mu)[1 + \mu + 2(1-\mu)\kappa] = \left[\frac{2\mu(1-\mu)(1+x^2\kappa)}{(1-\mu)x^2 + \mu(1-x)^2} - \mu - (1-\mu)(1+\kappa)\right]^2, \tag{B 1}$$

which can be rewritten as a second order polynomial in κ: $A_2\kappa^2 + A_1\kappa + A_0 = 0$, with:

$$A_0 = \frac{4\mu(1-\mu)(x-\mu)^2}{(x^2 - 2\mu x + \mu)^2}, \tag{B 2}$$

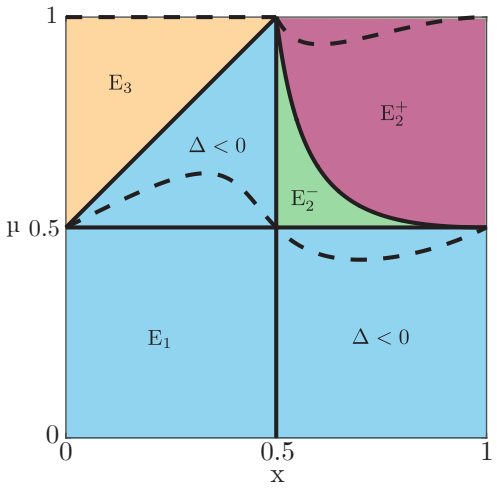

Figure 10. Plot of the different regions in the parameter space $(x, \mu) \in [0, 1]^2$ for the discussion of the roots of the equation $\Omega_r^2 = \Omega_\pm^2$. Plain lines delimit areas with different signs of the discriminant Δ and coefficient A_2. The sign of the coefficient A_1 is negative in between the two dashed lines. The coloured areas refer to position of Ω_r respectively to $\Omega_\pm$ (see figure 5d).

$$A_1 = \frac{4\mu(1-\mu)}{(x^2+2\mu x+\mu)^2}[x^2 + (1-2x-4x^2+2x^3)\mu - 2(1-3x+x^2)\mu^2], \tag{B 3}$$

and:

$$A_2 = -\frac{4\mu(1-\mu)^2x^2}{(x^2-2\mu x+\mu)^2}[(x^2+2x-1)\mu - x^2]. \tag{B 4}$$

The discriminant of this equation is thus given by:

$$\Delta = A_1^2 - 4A_0A_2 = \frac{16(1-\mu)^2}{(x^2-2\mu x+\mu)^2}(-1+2x)(-1+2\mu)(1+2x-2\mu), \tag{B 5}$$

and its roots by:

$$\kappa_\pm = \frac{-A_1 \pm \sqrt{\Delta}}{2A_2}. \tag{B 6}$$

Only positive roots are physical. A necessary condition is that the discriminant must be positive, else the roots are complex. From (B 5), we find that $\Delta < 0$ in two regions, labelled as such, in the parameter space $(x, \mu) \in [0, 1]^2$ (Fig. 10). If the discriminant is positive, the sign of the real roots is determined by the signs of A_0, A_1 and A_2, since $\kappa_-\kappa_+ = A_0/A_2$ and $\kappa_- + \kappa_+ = -A_1/A_2$. From (B 2), A_0 is positive, while from (B 4), the sign of A_2 is the sign of the quantity $x^2 - (x^2+2x-1)\mu$, which is positive except in the region denoted E_2^+ in Fig. 10, which is bounded by the bottom curve of equation $\mu = x^2/(x^2+2x-1)$ for $1/2 \le x \le 1$. Hence in this region, there is one positive root, which is κ_-. For $\kappa < \kappa_-$, we find that the ordering $\Omega_- < \Omega_r < \Omega_+$ holds, while for $\kappa > \kappa_-$, we find $\Omega_- < \Omega_+ < \Omega_r$. In the other regions, there are either no positive roots or two positive roots, respectively if A_1 is positive or negative. The sign of A_1 is given by the term in bracket in (B 3); it is found that $A_1 < 0$ between the two dashed curves in Fig. 10, and $A_1 > 0$ elsewhere. Hence, in the region denoted E_1, the two roots are negative, while the two roots are positive in regions E_2^- and E_3 (Fig. 10), with $\kappa_- < \kappa_+$. In these two regions, we find that the ordering $\Omega_- < \Omega_r < \Omega_+$ holds for $\kappa < \kappa_-$ and $\kappa > \kappa_+$. For $\kappa_- < \kappa < \kappa_+$, we find that $\Omega_- < \Omega_+ < \Omega_r$ in region E_2^-, and $\Omega_r < \Omega_- < \Omega_+$ in region E_3.

C. Suppression of the second negative band for large dissipation

To study dissipation, we substitute $K = K_r + \mathrm{i}K_i$ in the expression (2.4) of the effective mass. After some algebra, this yields:

$$m_{\text{eff}} = -\frac{\kappa}{(1+x^2\kappa)\Omega^2}\frac{(1-\Omega^2/\Omega_-^2)(1-\Omega^2/\Omega_+^2)+\mathrm{i}\alpha(1-\Omega^2/\kappa)}{1+\mathrm{i}\alpha-\Omega^2/\Omega_r^2}, \tag{C 1}$$

provided κ is redefined as $\kappa = K'/K_r$ [compare to (5.3)]. Apart from this redefinition, the other quantities are defined as previously, in particular $\Omega_\pm$ is given by (5.15) and Ω_r by (5.16). Hence at large dissipation, the effective mass has the following limit:

$$\lim_{\alpha\to\infty} m_{\text{eff}} = -\frac{\kappa}{(1+x^2\kappa)\Omega^2}\frac{1-\Omega^2/\kappa}{\Omega^2}.$$

This large-dissipation effective mass displays a single, low-frequency negative band, for $\Omega^2 < \kappa$ (and its imaginary part disappears). Intuitively, the two masses are then forced to move at the same amplitude, which suppresses the effect of the spring constant K. Hence, the main effect of dissipation is to make the second negative band studied in Sec. 5(b) vanish for a certain critical value $\alpha_c(x,\mu,\kappa)$ of the dissipation parameter α. However, Eq. (C 1) is too complex to allow for an analytical prediction of α_c.